# Supporting Information

# Enhancing Electrocatalytic Hydrogen Evolution Efficiency: Tuning Catalyst Support Pore Size to Optimize Hydrogen Adsorption-Desorption Kinetics

Yong Zhou[a,b], Bin Yang[b], Bing Li[b]*, and Xiaoyang Liu[a]*

a. State Key Laboratory of Inorganic Synthesis and Preparative Chemistry, College of Chemistry, Jilin University, Changchun 130012, China.

b. Center for High Pressure Science and Technology Advanced Research, Changchun 130012, China.

* Corresponding authors: Xiaoyang Liu (liuxy@jlu.edu.cn); Bing Li (libing@hpstar.ac.cn).

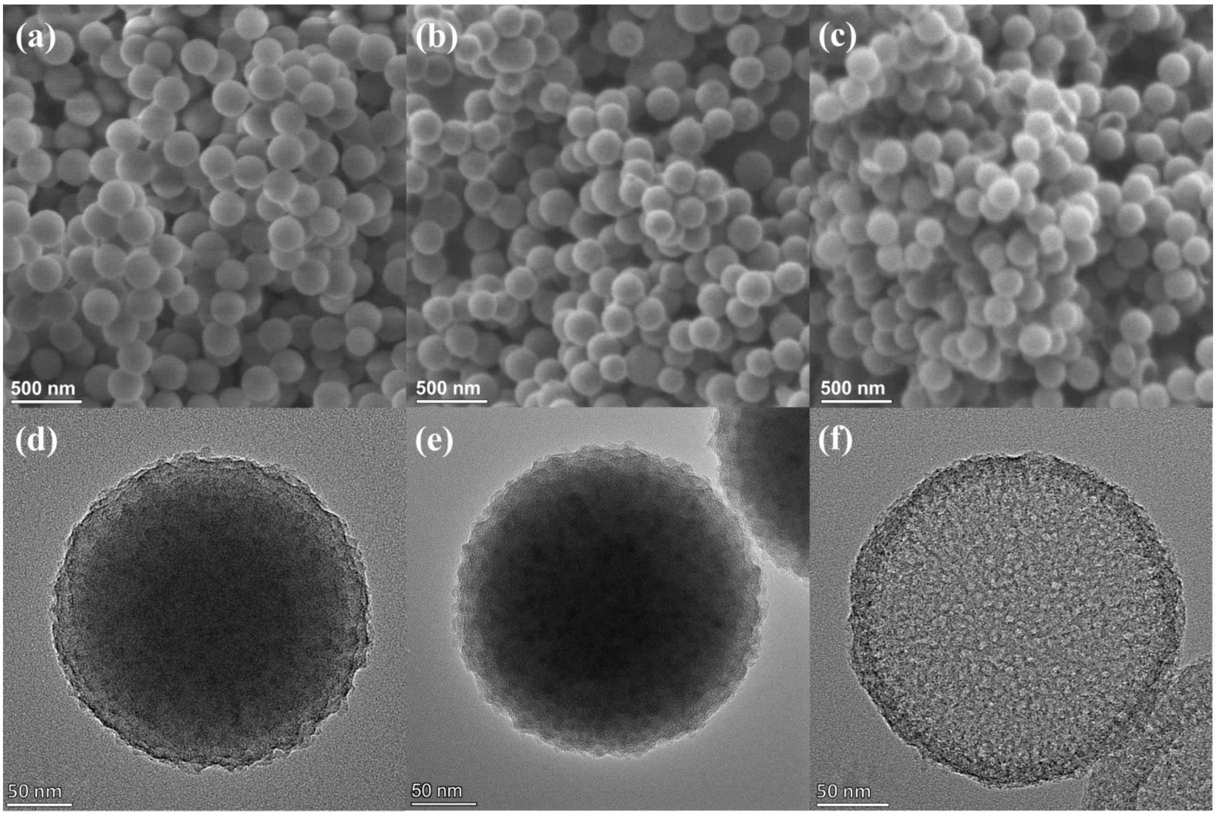


**Figure S1.** SEM images of (a) $SiO_2$@$SiO_2$/RF-1, (b) $SiO_2$@$SiO_2$/C-1, and (c) HMCS-1. TEM images of (d) $SiO_2$@$SiO_2$/RF-1, (e) $SiO_2$@$SiO_2$/C-1, and (f) HMCS-1.

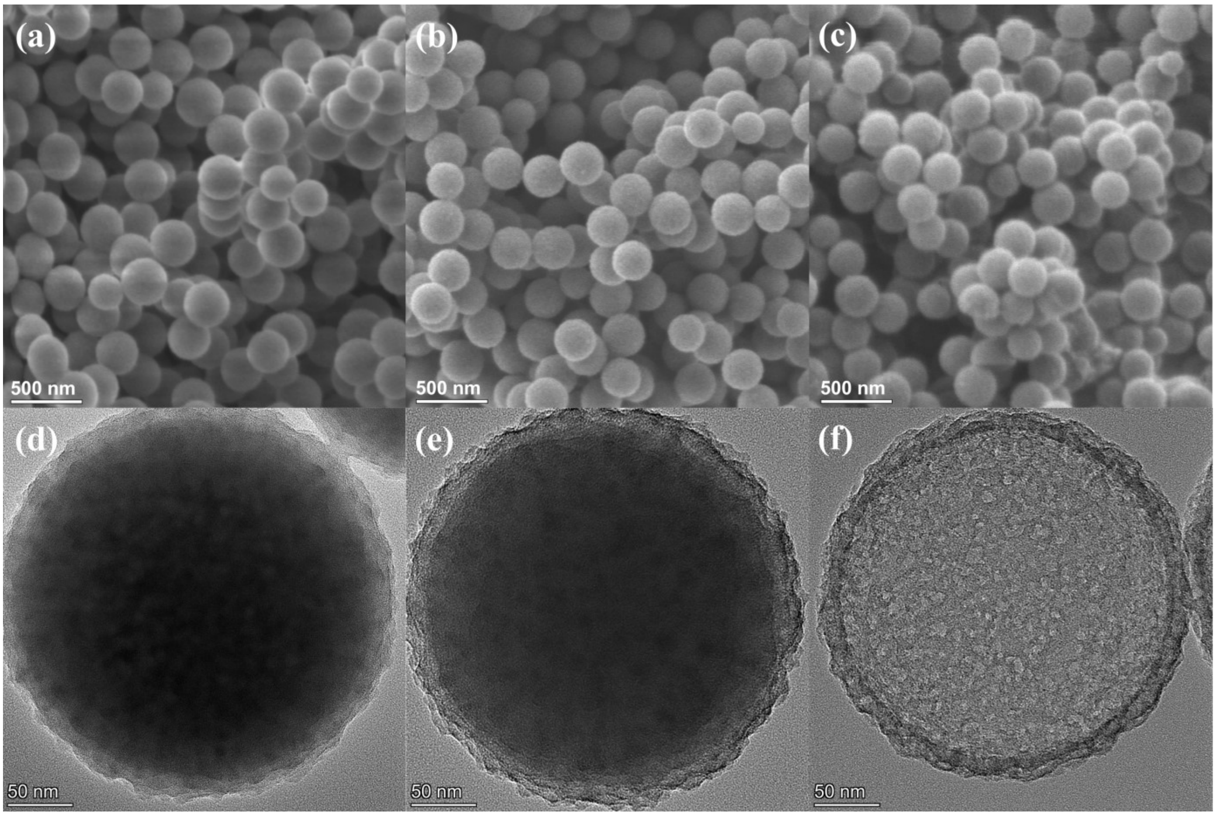


**Figure S2.** SEM images of (a) $SiO_2$@$SiO_2$/RF-2, (b) $SiO_2$@$SiO_2$/C-2, and (c) HMCS-2. TEM images of (d) $SiO_2$@$SiO_2$/RF-2, (e) $SiO_2$@$SiO_2$/C-2, and (f) HMCS-2.

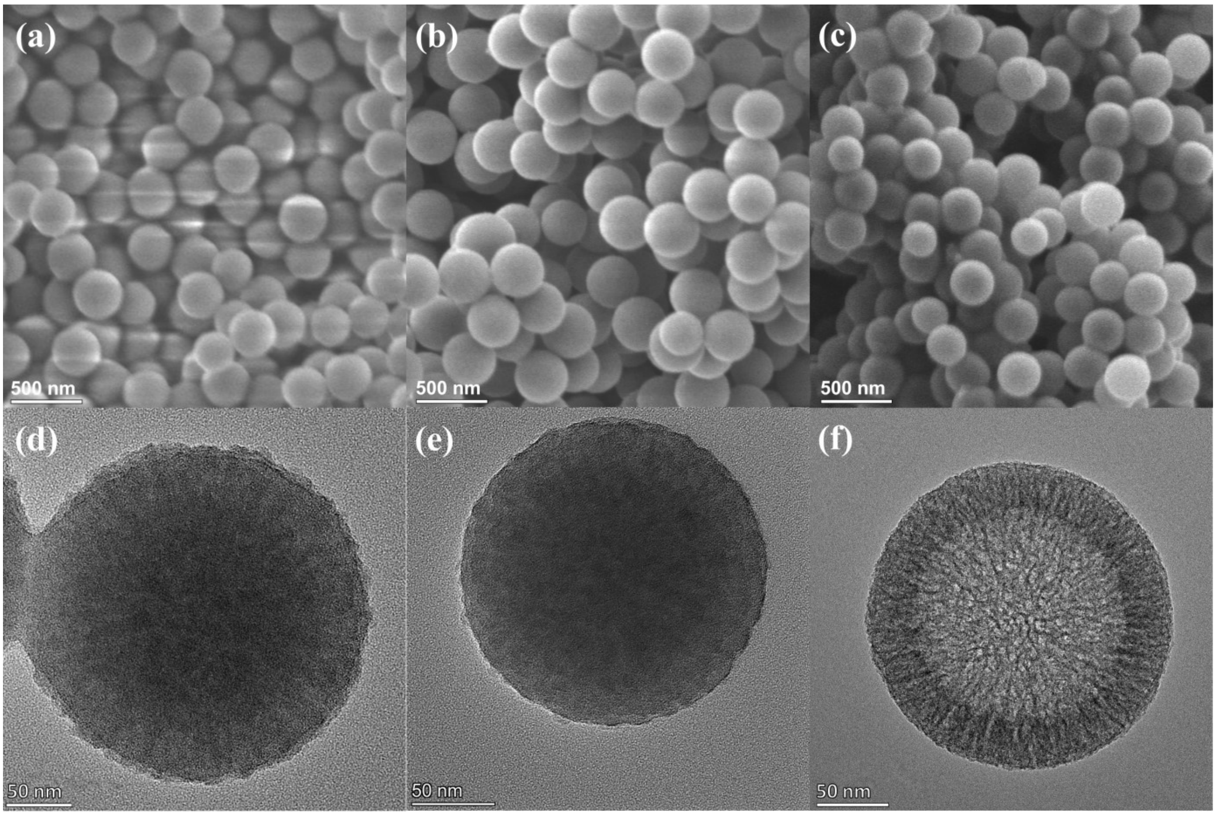


**Figure S3.** SEM images of (a) $SiO_2$@$SiO_2$/RF-3, (b) $SiO_2$@$SiO_2$/C-3, and (c) HMCS-3. TEM images of (d) $SiO_2$@$SiO_2$/RF-3, (e) $SiO_2$@$SiO_2$/C-3, and (f) HMCS-3.

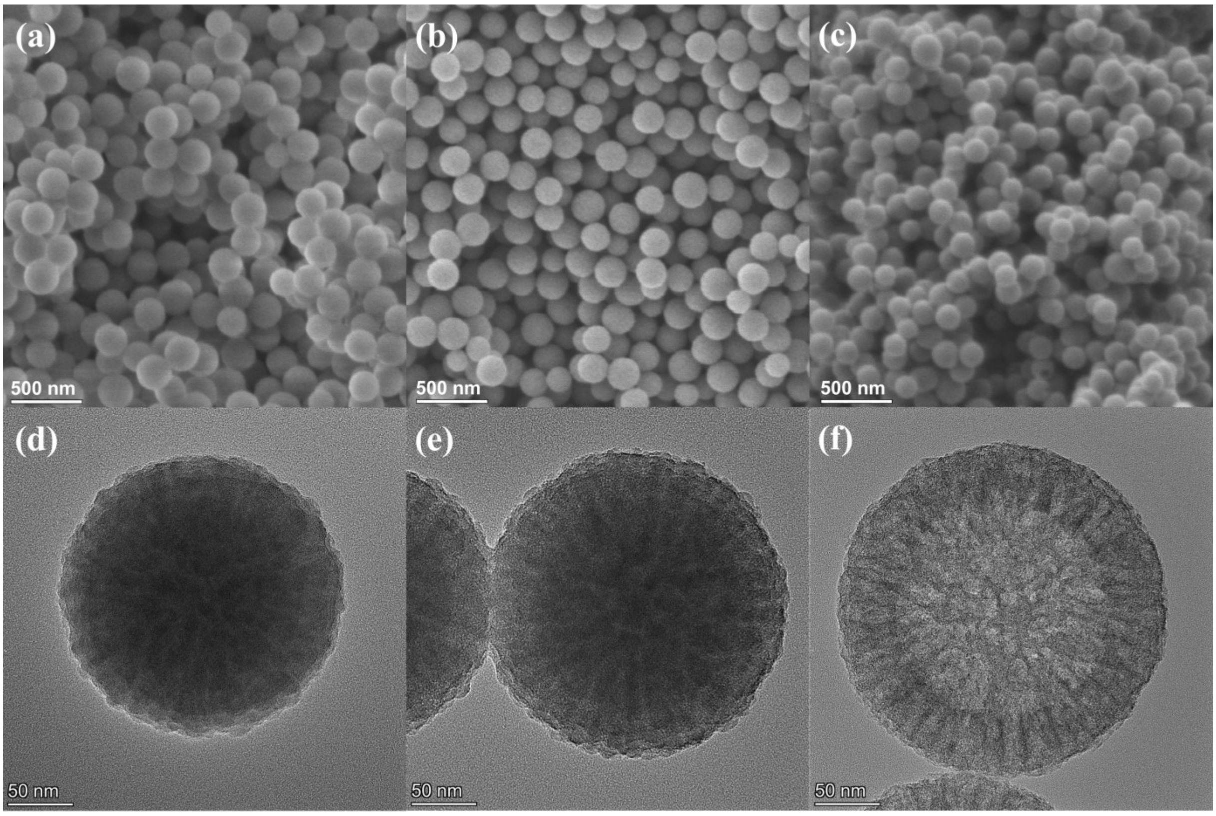


**Figure S4.** SEM images of (a) $SiO_2$@$SiO_2$/RF-4, (b) $SiO_2$@$SiO_2$/C-4, and (c) HMCS-4. TEM images of (d) $SiO_2$@$SiO_2$/RF-4, (e) $SiO_2$@$SiO_2$/C-4, and (f) HMCS-4.

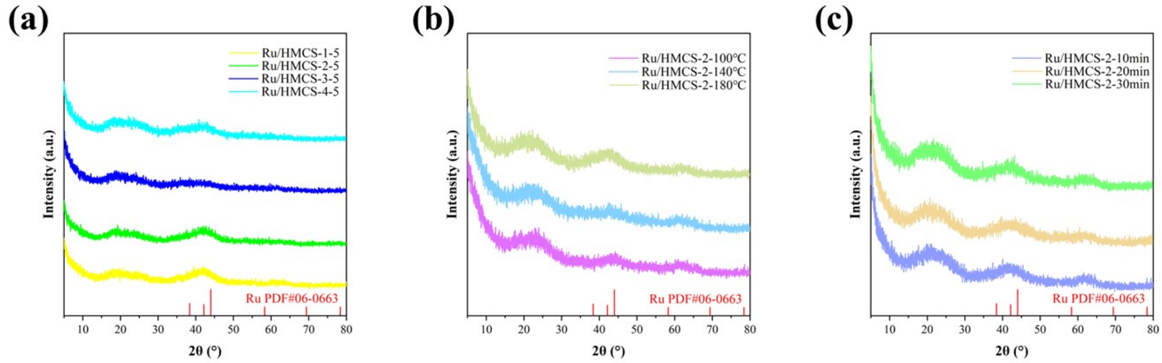


**Figure S5.** XRD patterns of Ru/HMCS-1-5, Ru/HMCS-2-5, Ru/HMCS-3-5 and Ru/HMCS-4-5 (a); Ru/HMCS-2-100℃, Ru/HMCS-2-140℃ and Ru/HMCS-2-180℃ (b); Ru/HMCS-2-10min, Ru/HMCS-2-20min and Ru/HMCS-2-30min (c).

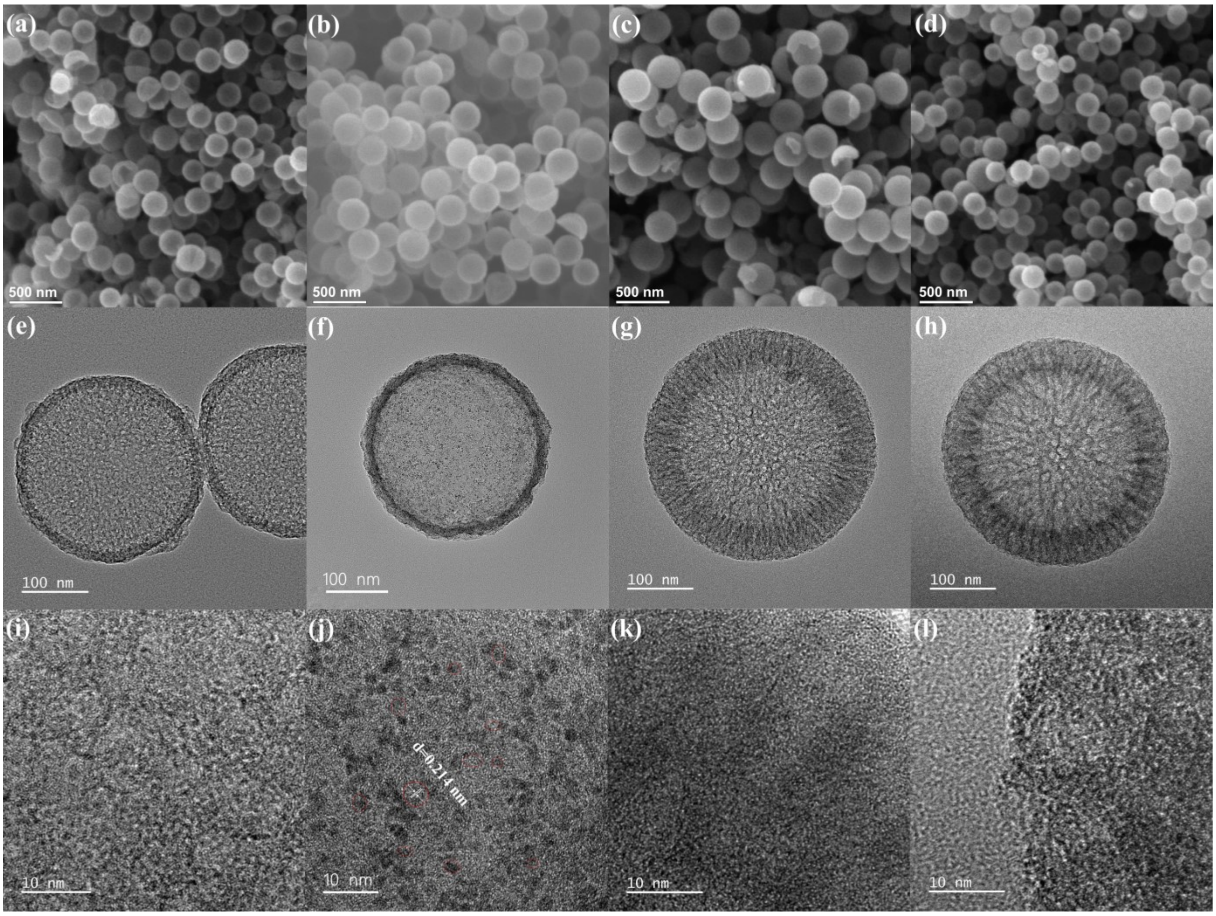


**Figure S6.** SEM images of (a) Ru/HMCS-1-5, (b) Ru/HMCS-2-5, (c) Ru/HMCS-3-5, and (d) Ru/HMCS-4-5. TEM images of (e) Ru/HMCS-1-5, (f) Ru/HMCS-2-5, (g) Ru/HMCS-3-5, and (h) Ru/HMCS-4-5. HRTEM images of (i) Ru/HMCS-1-5, (j) Ru/HMCS-2-5, (k) Ru/HMCS-3-5 and (l) Ru/HMCS-4-5.

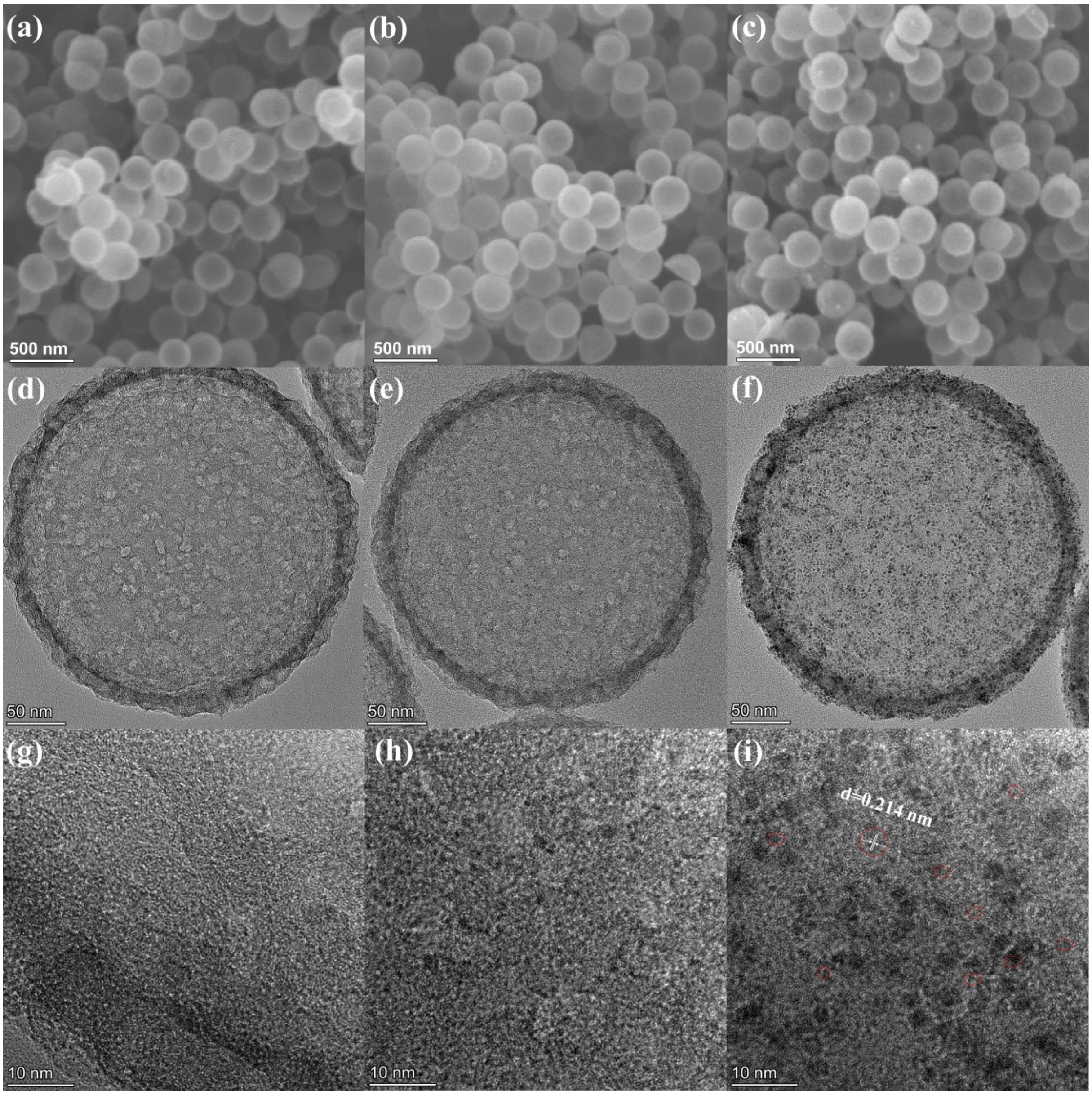


**Figure S7.** SEM images of Ru/HMCS-2-0 (a), Ru/HMCS-2-1 (b), and Ru/HMCS-2-7 (c). TEM images of Ru/HMCS-2-0 (d), Ru/HMCS-2-1 (e), and Ru/HMCS-2-7 (f). HRTEM images of Ru/HMCS-2-0 (g), Ru/HMCS-2-1 (h), and Ru/HMCS-2-7 (i).

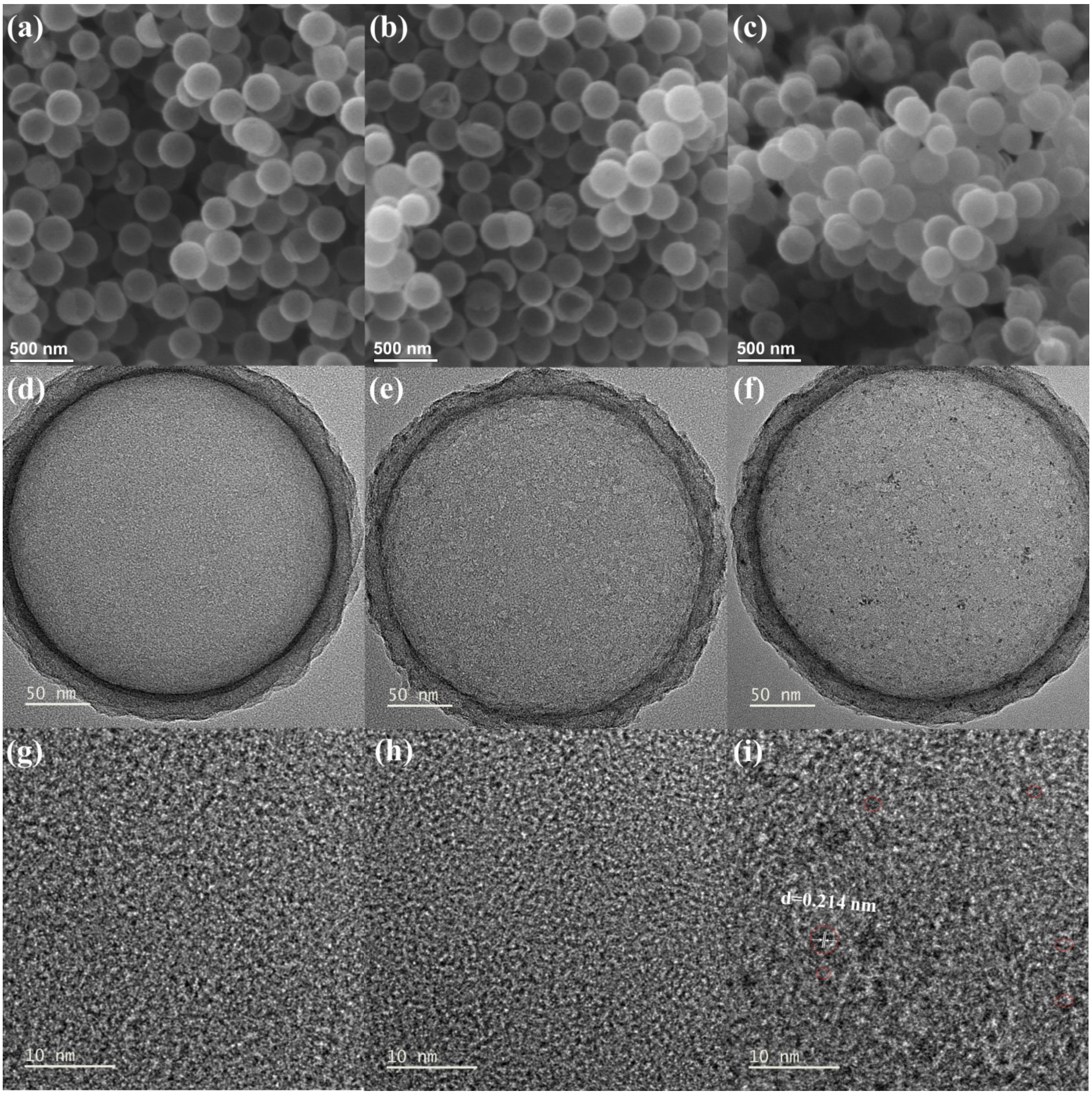


**Figure S8.** SEM images of Ru/HMCS-2-100℃ (a), Ru/HMCS-2-140℃ (b), and Ru/HMCS-2-180℃ (c). TEM images of Ru/HMCS-2-100℃ (d), Ru/HMCS-2-140℃ (e), and Ru/HMCS-2-180℃ (f). HRTEM images of Ru/HMCS-2-100℃ (g), Ru/HMCS-2-140℃ (h), and Ru/HMCS-2-180℃ (i).

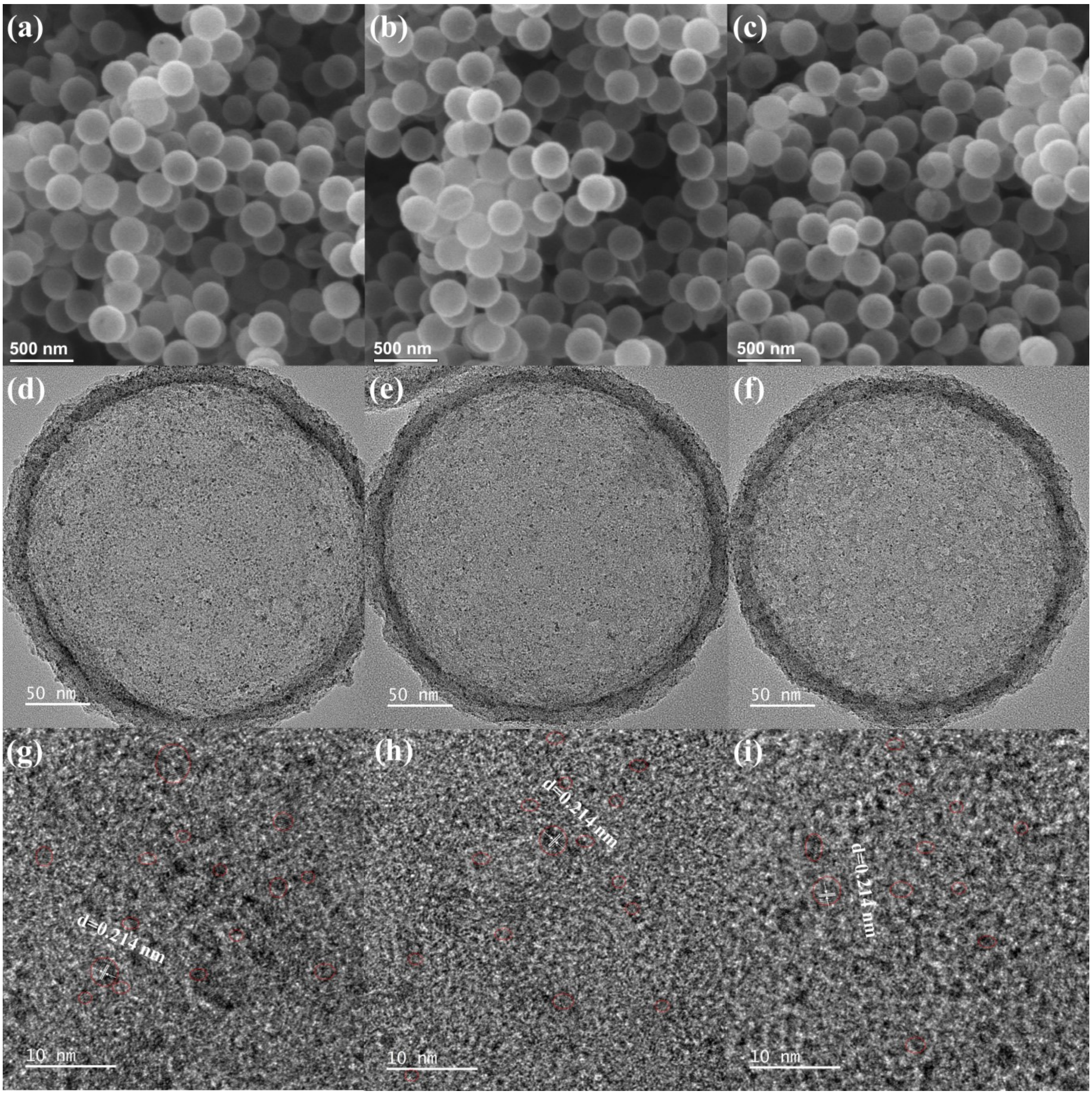


**Figure S9.** SEM images of Ru/HMCS-2-10min (a), Ru/HMCS-2-20min (b), and Ru/HMCS-2-30min (c). TEM images of Ru/HMCS-2-10min (d), Ru/HMCS-2-20min (e), and Ru/HMCS-2-30min (f). HRTEM images of Ru/HMCS-2-10min (g), Ru/HMCS-2-20min (h), and Ru/HMCS-2-30min (i).

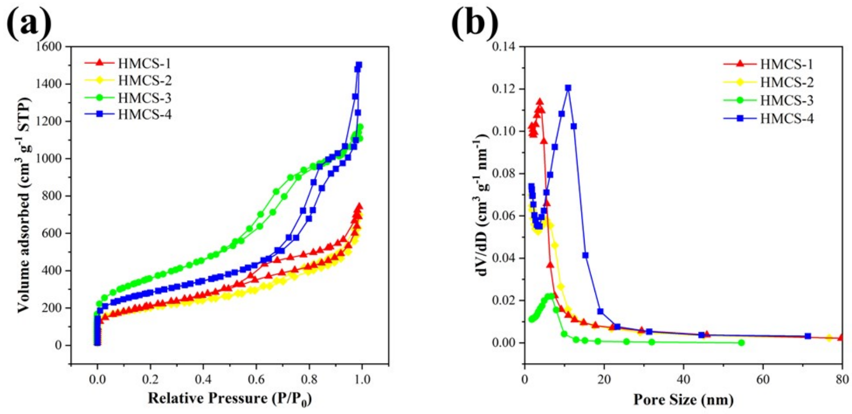


**Figure S10.** (a) $N_2$-adsorption/desorption isotherms and (b) pore size distribution of HMCSs.

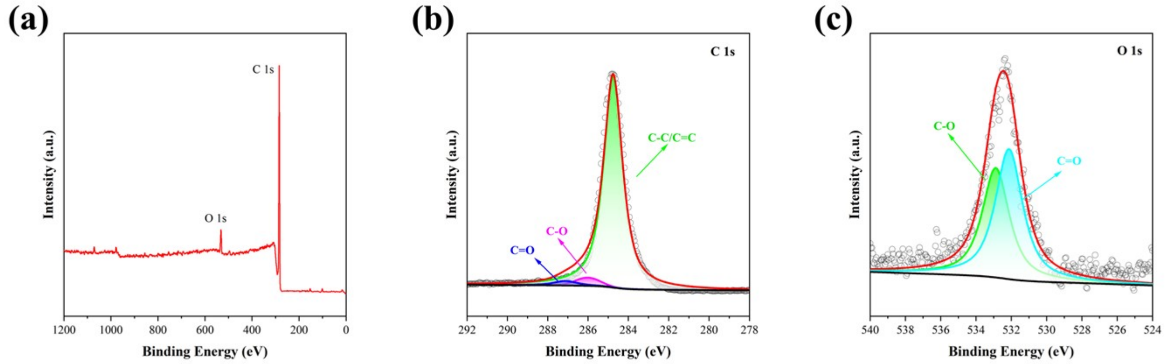


**Figure S11.** (a) XPS survey spectrum of HMCS-2. High-resolution XPS spectra of C 1*s* (b) and O 1*s* (c) for HMCS-2.

**Table S1.** The Ru content of the samples by ICP-OES.

| Catalyst | Ru (*wt*%) |
|---|---|
| Ru/HMCS-1-5 | 2.83 |
| Ru/HMCS-2-5 | 3.12 |
| Ru/HMCS-3-5 | 2.51 |
| Ru/HMCS-4-5 | 2.34 |
| Ru/HMCS-2-1 | 1.15 |
| Ru/HMCS-2-3 | 2.42 |
| Ru/HMCS-2-7 | 5.78 |
| Ru/HMCS-2-100℃ | 1.98 |
| Ru/HMCS-2-140℃ | 2.04 |
| Ru/HMCS-2-180℃ | 2.23 |
| Ru/HMCS-2-10min | 2.25 |
| Ru/HMCS-2-20min | 2.97 |
| Ru/HMCS-2-30min | 4.33 |

**Table S2.** Electrocatalytic Performance for the HER of Ru/HMCS and commercial Pt/C catalysts

| Catalyst | $\eta_{10}$ (mV) | Tafel slope (mV dec$^{-1}$) | $C_{dl}$ (mF cm$^{-2}$) | ECSA (cm$^2$) |
|---|---|---|---|---|
| Ru/HMCS-1-5 | 30.9 | 47.00 | 25.80 | 45.60 |
| Ru/HMCS-2-5 | 22.0 | 48.34 | 33.74 | 59.64 |
| Ru/HMCS-3-5 | 29.8 | 47.57 | 24.24 | 42.84 |
| Ru/HMCS-4-5 | 23.7 | 43.55 | 29.66 | 52.42 |
| Ru/HMCS-2-1 | 36.5 | 66.39 | 38.39 | 67.85 |
| Ru/HMCS-2-3 | 18.9 | 39.54 | 39.66 | 70.10 |
| Ru/HMCS-2-7 | 21.1 | 43.67 | 40.48 | 71.55 |
| Ru/HMCS-2-100℃ | 83.3 | 158.45 | 25.43 | 44.95 |
| Ru/HMCS-2-140℃ | 67.9 | 122.59 | 26.93 | 47.60 |
| Ru/HMCS-2-180℃ | 46.9 | 121.68 | 37.29 | 65.91 |
| Ru/HMCS-2-10min | 32.2 | 70.68 | 41.02 | 72.50 |
| Ru/HMCS-2-20min | 37.3 | 101.39 | 39.43 | 69.69 |
| Ru/HMCS-2-30min | 31.2 | 78.17 | 37.29 | 65.91 |
| 20 *wt.*%Pt/C | 31.9 | 57.03 | 50.30 | 88.91 |
| 40 *wt.*%Pt/C | 21.2 | 41.21 | 55.62 | 98.31 |

**Table S3.** Fitted EIS results of Ru/HMCS catalysts

| Catalyst | $R_s$ (Ω) | $R_{ct}$ (Ω) |
|---|---|---|
| Ru/HMCS-1-5 | 14.75 | 46.24 |
| Ru/HMCS-2-5 | 17.91 | 18.59 |
| Ru/HMCS-3-5 | 22.21 | 38.32 |
| Ru/HMCS-4-5 | 15.79 | 39.49 |
| Ru/HMCS-2-1 | 14.76 | 64.26 |
| Ru/HMCS-2-3 | 13.83 | 18.13 |
| Ru/HMCS-2-7 | 13.75 | 8.72 |
| Ru/HMCS-2-100℃ | 15.81 | 113.6 |
| Ru/HMCS-2-140℃ | 34.54 | 95.02 |
| Ru/HMCS-2-180℃ | 32.9 | 78.59 |
| Ru/HMCS-2-10min | 21.18 | 86.79 |
| Ru/HMCS-2-20min | 16.82 | 55.21 |
| Ru/HMCS-2-30min | 15.97 | 29.42 |

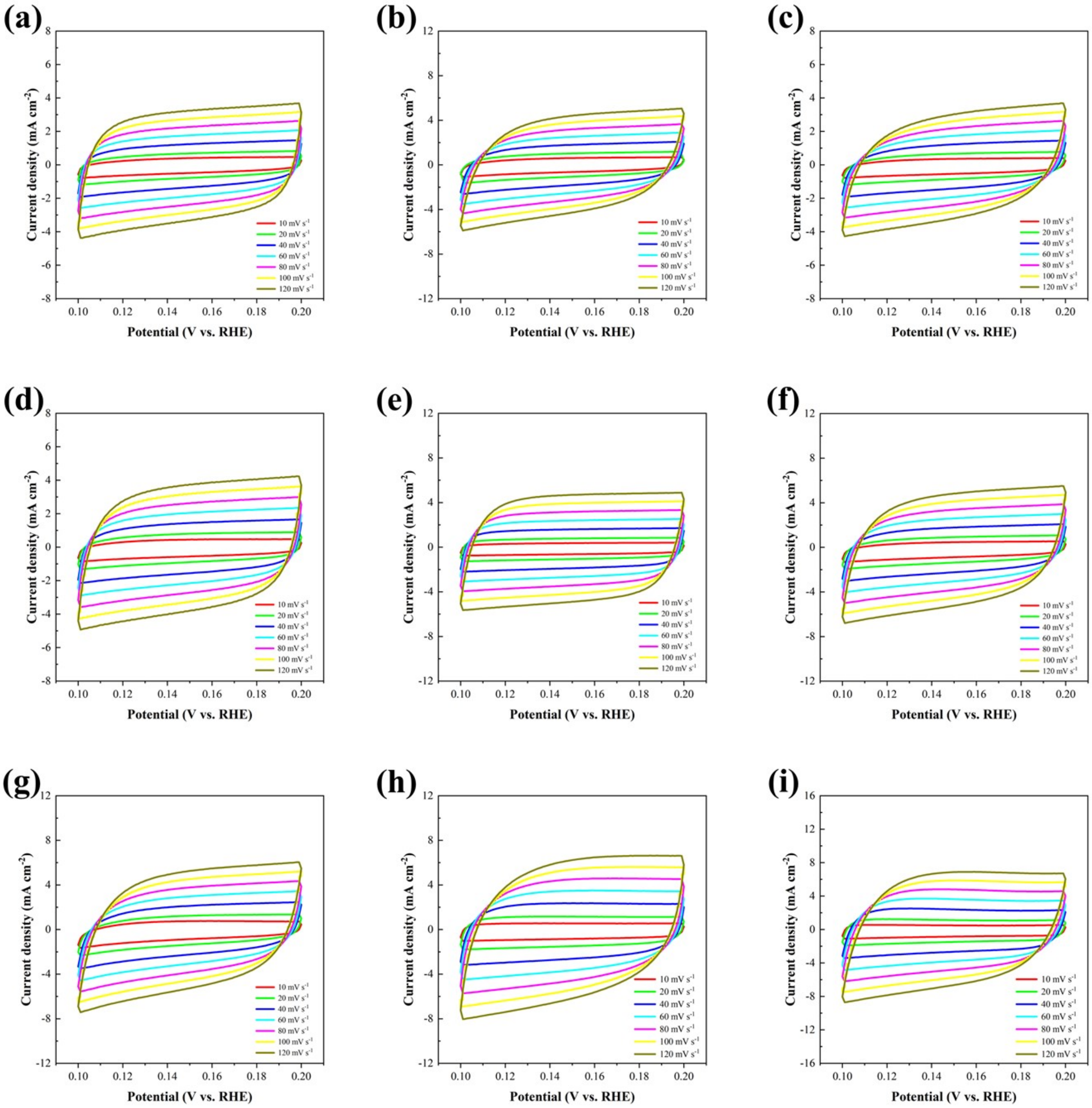


**Figure S12.** Cyclic voltammetry curves of Ru/HMCS-1-5 (a), Ru/HMCS-2-5 (b), Ru/HMCS-3-5 (c), Ru/HMCS-4-5 (d), Ru/HMCS-2-1 (e), Ru/HMCS-2-3 (f), Ru/HMCS-2-7 (g), 20 *wt*.%Pt/C (h) and 40 *wt*.%Pt/C (i) (10−120 mV $s^{-1}$, in 1.0 M KOH solution).

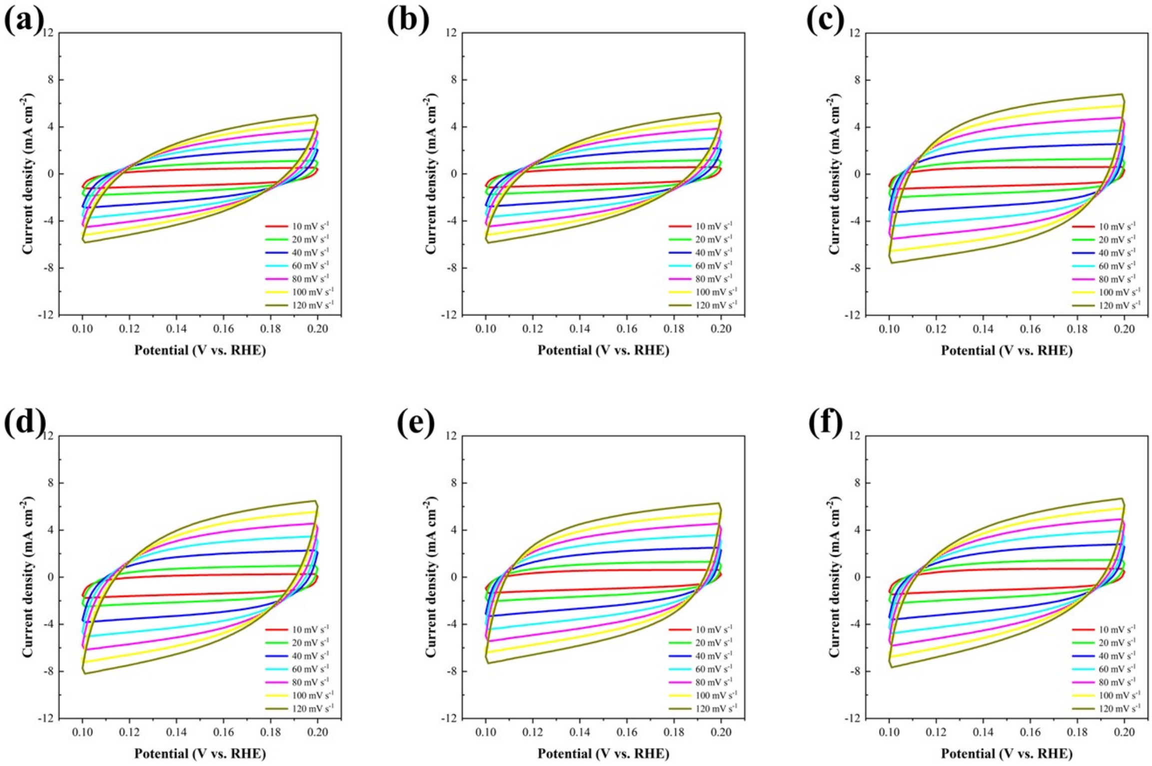


**Figure S13.** Cyclic voltammetry curves of Ru/HMCS-2-100℃ (a), Ru/HMCS-2-140℃ (b), Ru/HMCS-2-180℃ (c), Ru/HMCS-2-10min (d), Ru/HMCS-2-20min (e) and Ru/HMCS-2-30min (f) (10−120 mV $s^{-1}$, in 1.0 M KOH solution).

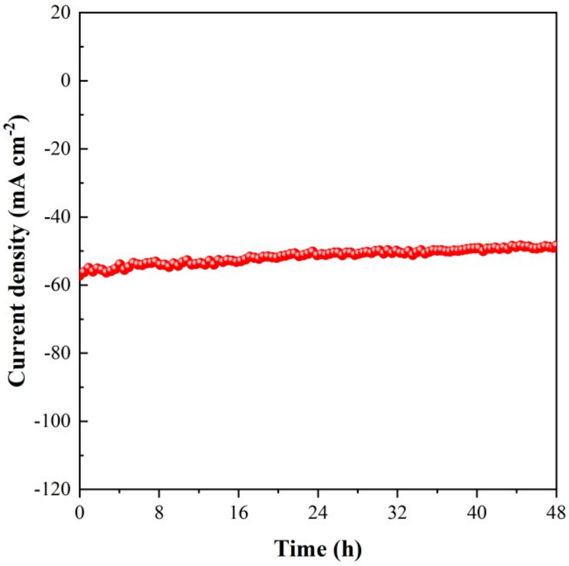


**Figure S14.** Chronoamperometric measurement of Ru/HMCS-2-3 in 1.0 M KOH.

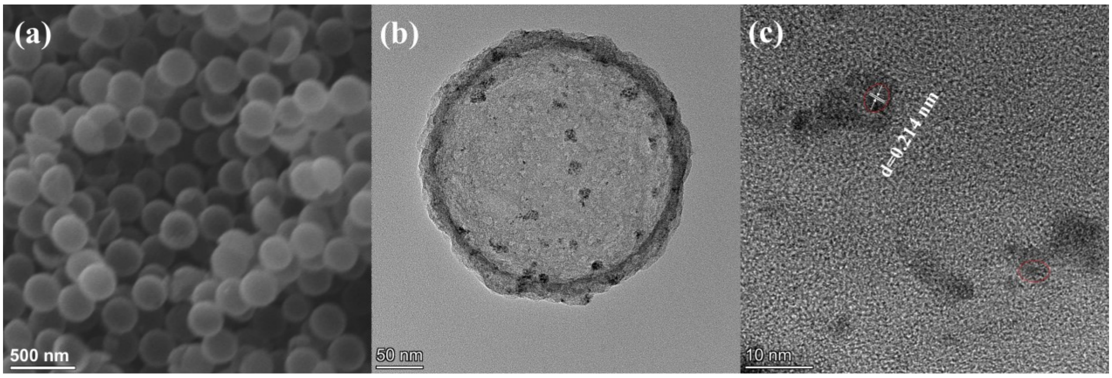


**Figure S15.** Characterizations of Ru/HMCS-2-3 catalyst after 48 h chronoamperometric measurement. (a) SEM image, (b) TEM image, and (c) HRTEM image.

**Table S4.** Comparison of HER activity of Ru/HMCS-2-3 catalyst with recently reported representative Ru-based catalysts in 1.0 M KOH solution.

| Catalyst | Ru content (wt.%) | $\eta_{10}$ (mV) | Tafel slope (mV dec$^{-1}$) | $R_{ct}$ ($\Omega$) | Ref. |
|---|---|---|---|---|---|
| Ru/HMCS-2-3 | 2.42 | 18.9 | 39.54 | 18.1 | This work |
| $Ru_{90}Ni_{10}$/rGOP | 94 | 6 | 26 | 1.4 | [1] |
| Ru/C-20A | 85.5 | 13 | 35 | —— | [2] |
| UP-RuNi$_{SAs}$/C | —— | 9 | 37.6 | 0.10 | [3] |
| Ru/NC | 5.83 | 24 | 29 | —— | [4] |
| Ru$_{NP}$/Ru$_{SA}$@CFN-800 | 12 | 33 | 37.16 | 31.91 | [5] |
| CNT-V-Fe-Ru | 17.84 | 38 | 41 | 24.6 | [6] |
| NMC Ru$_{SA+NC}$ | 2.0 | 5 | 136 | —— | [7] |
| α-Ru@Co-DHC | —— | 40 | 62 | —— | [8] |
| Ru$_{1+NPs}$/N-C-700℃ | 7.57 | 39 | 27.6 | 29.97 | [9] |
| Ru/Co-N-C-800℃ | 0.36 | 17 | 27.8 | —— | [10] |
| Ru/3d-OMC | —— | 20 | 40.5 | —— | [11] |
| Ru S/DA | —— | 58 | 90 | —— | [12] |
| Ru$_{1,n}$-NC | 7.1 | 14.8 | 22.4 | —— | [13] |
| Ru$_{NP}$@RuN$_x$-OFC/NC | 17.84 | 19 | 35.35 | 10.81 | [14] |
| $Ru_{55}$@CN | 1.728 | 36 | 39 | —— | [15] |
| Ru$_{SA+NP}$/DC | 11.8 | 18.8 | 35.8 | —— | [16] |
| NiRu$_{0.13}$-BDC | —— | 34 | 32 | —— | [17] |
| Ru/Co@OG | 6.9 | 13 | 22.8 | —— | [18] |
| $Ru_1$CoP/CDs−1000 | 13.69 | 51 | 73.4 | —— | [19] |
| Ru/g-$C_3N_4$-C-$TiO_2$ | 12.4 | 107 | 83 | 58 | [20] |
| Ru/p-NC | 1.0 | 10 | 17 | 4.7 | [21] |
| Ru/$MoO_2$ | 21.26 | 16 | 32 | 24.59 | [22] |

| | | | | | |
|---|---|---|---|---|---|
| Ru/g-$C_3N_4$–2 | 3.27 | 34 | 27 | 35.2 | [23] |
| Ru-CoP/NC | —— | 22 | 50 | —— | [24] |
| Ru ADC | —— | 18 | 41 | —— | [25] |
| ECM@Ru | 0.68 | 83 | 58 | 15.1 | [26] |
| Ru-N/BC | 0.46 | 51 | 44 | 20.3 | [27] |
| Ru-NPs/SAs@N-TC | 0.457 | 97 | 58 | —— | [28] |
| Ru-NMCNs-500 | 3.04 | 39 | 35.2 | 8.86 | [29] |
| Ru@CNT-500 | 0.068 | 36.69 | 28.82 | —— | [30] |
| 5%Ru-$MoS_2$/CNT | 5 (*at.*%) | 50 | 62 | —— | [31] |
| $RuS_x$/S-GO | 44.31 | 58 | 56 | —— | [32] |

# Reference


1. Y. Liu, H. Shi, T. Y. Dai, S. P. Zeng, G. F. Han, T. H. Wang, Z. Wen, X. Y. Lang and Q. Jiang, In situ engineering multifunctional active sites of ruthenium-nickel alloys for pH-universal ampere-level current-density hydrogen evolution, *Small*, 2024, **20**, 2311509.
2. B. H. Cui, H. Zhu, M. Wang, J. R. Zeng, J. F. Zhang, Z. L. Tian, C. L. Jiang, Z. J. Sun, H. T. Yang, Y. Liu, J. Ding, Z. Y. Luo, Y. N. Chen, W. Chen and W. B. Hu, Intermediate state of dense Ru assembly captured by high-temperature shock for durable ampere-level hydrogen production, *ACS Mater. Lett.*, 2024, **6**, 1532-1541.
3. R. Yao, K. A. Sun, K. Y. Zhang, Y. Wu, Y. J. Du, Q. Zhao, G. Liu, C. Chen, Y. H. Sun and J. P. Li, Stable hydrogen evolution reaction at high current densities *via* designing the Ni single atoms and Ru nanoparticles linked by carbon bridges, *Nat. Commun.*, 2024, **15**, 2218.
4. Y. P. Zhu, K. Fan, C. S. Hsu, G. Chen, C. S. Chen, T. C. Liu, Z. Z. Lin, S. X. She, L. Q. Li, H. M. Zhou, Y. Zhu, H. M. Chen and H. T. Huang, Supported ruthenium single-atom and clustered catalysts outperform benchmark Pt for alkaline hydrogen evolution, *Adv. Mater.*, 2023, **35**, 2301133.
5. T. M. Luo, J. F. Huang, Y. Z. Hu, C. K. Yuan, J. S. Chen, L. Y. Cao, K. Kajiyoshi, Y. J. Liu, Y. Zhao, Z. J. Li and Y. Q. Feng, Fullerene lattice-confined Ru nanoparticles and single atoms synergistically boost electrocatalytic hydrogen evolution reaction, *Adv. Funct. Mater.*, 2023, **33**, 2213058.
6. T. T. Gao, X. M. Tang, X. Q. Li, S. W. Wu, S. M. Yu, P. P. Li, D. Xiao and Z. Y. Jin, Understanding the atomic and defective interface effect on ruthenium clusters for the hydrogen evolution reaction, *ACS Catal.*, 2023, **13**, 49-59.
7. H. X. Yao, X. K. Wang, K. Li, C. Li, C. H. Zhang, J. Zhou, Z. W. Cao, H. L. Wang, M. Gu, M. H. Huang and H. Q. Jiang, Strong electronic coupling between ruthenium single atoms and ultrafine nanoclusters enables economical and effective hydrogen production, *Appl. Catal. B-Environ.*, 2022, **312**, 121378.
8. W. X. Yang, W. Y. Zhang, R. Liu, F. Lv, Y. G. Chao, Z. C. Wang and S. J. Guo, Amorphous Ru nanoclusters onto Co-doped 1D carbon nanocages enables efficient hydrogen evolution catalysis, *Chin. J. Catal.*, 2022, **43**, 110-115.
9. S. R. Wang, M. M. Wang, Z. Liu, S. J. Liu, Y. J. Chen, M. Li, H. Zhang, Q. K. Wu, J. H. Guo, X. Q. Feng, Z. Chen and Y. Pan, Synergetic function of the single-atom Ru-$N_4$ site and Ru nanoparticles for hydrogen production in a wide pH range and seawater electrolysis, *ACS Appl. Mater. Interfaces*, 2022, **14**, 15250-15258.
10. C. L. Rong, X. J. Shen, Y. Wang, L. Thomsen, T. W. Zhao, Y. B. Li, X. Y. Lu, R. Amal and C. Zhao, Electronic structure engineering of single-atom Ru sites *via* Co-$N_4$ Sites for bifunctional pH-universal water splitting, *Adv. Mater.*, 2022, **34**, 2110103.
11. Z. H. Liu, Y. Du, R. H. Yu, M. B. Zheng, R. Hu, J. S. Wu, Y. Y. Xia, Z. C. Zhuang and D. S. Wang, Tuning mass transport in electrocatalysis down to sub-5 nm through nanoscale grade separation, *Angew. Chem. Int. Edit.*, 2022, **62**, e2022126.
12. Y. Liu, N. Chen, W. D. Li, M. Z. Sun, T. Wu, B. L. Huang, X. Yong, Q. H. Zhang, L. Gu, H. Q. Song, R. Bauer, J. S. Tse, S. Q. Zang, B. Yang and S. Y. Lu, Engineering the synergistic effect of carbon dots-stabilized atomic and subnanometric ruthenium as highly efficient electrocatalysts for robust hydrogen evolution, *Smartmat*, 2022, **3**, 249-259.
13. Q. He, Y. Z. Zhou, H. W. Shou, X. Y. Wang, P. J. Zhang, W. J. Xu, S. C. Qiao, C. Q. Wu, H. J. Liu, D. B. Liu, S. M. Chen, R. Long, Z. M. Qi, X. J. Wu and L. Song, Synergic reaction kinetics over adjacent ruthenium sites for superb hydrogen generation in alkaline media, *Adv. Mater.*, 2022, **34**, 2110604.
14. Y. Q. Feng, W. H. Feng, J. Wan, J. S. Chen, H. Wang, S. M. Li, T. M. Luo, Y. Z. Hu, C. K. Yuan, L. Y. Cao, L. L. Feng, J. Li, R. Wen and J. F. Huang, Spherical *vs*. planar: Steering the electronic communication between Ru nanoparticle and single atom to boost the electrocatalytic hydrogen evolution activity both in acid and alkaline, *Appl. Catal. B-Environ.*, 2022, **307**, 121193.

15. S. Ajmal, T. D. H. Bui, Q. V. Bui, T. Yang, X. D. Shao, A. Kumar, S.-G. Kim and H. Lee, Accelerating water reduction towards hydrogen generation via cluster size adjustment in Ru-incorporated carbon nitride, *Chem. Eng. J.*, 2022, **429**, 132282.
16. L. J. Zhang, H. Jang, Y. Wang, Z. Li, W. Zhang, M. G. Kim, D. J. Yang, S. G. Liu, X. Liu and J. Cho, Exploring the dominant role of atomic- and nano-ruthenium as active sites for hydrogen evolution reaction in both acidic and alkaline media, *Adv. Sci.*, 2021, **8**, 2004516.
17. Y. Sun, Z. Xue, Q. Liu, Y. Jia, Y. Li, K. Liu, Y. Lin, M. Liu, G. Li and C. Y. Su, Modulating electronic structure of metal-organic frameworks by introducing atomically dispersed Ru for efficient hydrogen evolution, *Nat. Commun.*, 2021, **12**, 1369.
18. P. Su, W. Pei, X. Wang, Y. Ma, Q. Jiang, J. Liang, S. Zhou, J. Zhao, J. Liu and G. Q. Lu, Exceptional electrochemical HER performance with enhanced electron transfer between Ru nanoparticles and single atoms dispersed on a carbon substrate, *Angew. Chem. Int. Edit.*, 2021, **60**, 16044-16050.
19. H. Song, M. Wu, Z. Tang, J. S. Tse, B. Yang and S. Lu, Single atom ruthenium-doped CoP/CDs nanosheets *via* splicing of carbon-dots for robust hydrogen production, *Angew. Chem. Int. Edit.*, 2021, **60**, 7234-7244.
20. Z. Li, Y. Yang, S. Wang, L. Gu and S. Shao, High-density ruthenium single atoms anchored on oxygen-vacancy-rich g-$C_3N_4$-C-$TiO_2$ heterostructural nanosphere for efficient electrocatalytic hydrogen evolution reaction, *ACS Appl. Mater. Interfaces*, 2021, **13**, 46608-46619.
21. Y. Li, H. Liu, B. Li, Z. Yang, Z. Guo, J. B. He, J. Xie and T. C. Lau, Ru single atoms and nanoclusters on highly porous N-doped carbon as a hydrogen evolution catalyst in alkaline solutions with ultrahigh mass activity and turnover frequency, *J. Mater. Chem. A*, 2021, **9**, 12196-12202.
22. H. Li, K. Liu, J. Fu, K. Chen, K. Yang, Y. Lin, B. Yang, Q. Wang, H. Pan, Z. Cai, H. Li, M. Cao, J. Hu, Y.-R. Lu, T.-S. Chan, E. Cortes, A. Fratalocchi and M. Liu, Paired Ru-O-Mo ensemble for efficient and stable alkaline hydrogen evolution reaction, *Nano Energy*, 2021, **82**, 105767.
23. D. Li, Y. Liu, Z. Liu, J. Yang, C. Hu and L. Feng, Electrochemical hydrogen evolution reaction efficiently catalyzed by Ru-N coupling in defect-rich Ru/g-$C_3N_4$ nanosheets, *J. Mater. Chem. A*, 2021, **9**, 15019-15026.
24. Y. Hao, H. Xue, J. Sun, N. Guo, T. Song, J. Sun and Q. Wang, Tuning the electronic structure of CoP embedded in N-doped porous carbon nanocubes *via* Ru doping for efficient hydrogen evolution, *ACS Appl. Mater. Interfaces*, 2021, **13**, 56035-56044.
25. D. Cao, J. Wang, H. Xu and D. Cheng, Construction of dual-site atomically dispersed electrocatalysts with Ru-$C_5$ single atoms and Ru-$O_4$ nanoclusters for accelerated alkali hydrogen evolution, *Small*, 2021, **17**, 2101163.
26. H. Zhang, W. Zhou, F. Lu Xue, T. Chen and W. Lou Xiong, Implanting isolated Ru atoms into edge-rich carbon matrix for efficient electrocatalytic hydrogen evolution, *Adv. Energy Mater.*, 2020, **10**, 2000882.
27. Y. Yu, S. Yang, M. Dou, Z. Zhang and F. Wang, Photochemically activated atomic ruthenium supported on boron-doped carbon as a robust electrocatalyst for hydrogen evolution, *J. Mater. Chem. A*, 2020, **8**, 16669-16675.
28. B. Yan, D. Liu, X. Feng, M. Shao and Y. Zhang, Ru species supported on MOF-derived N-doped $TiO_2$/C hybrids as efficient electrocatalytic/photocatalytic hydrogen evolution reaction catalysts, *Adv. Funct. Mater.*, 2020, **30**, 2003007.
29. J. Peng, Y. Chen, K. Wang, Z. Tang and S. Chen, High-performance Ru-based electrocatalyst composed of Ru nanoparticles and Ru single atoms for hydrogen evolution reaction in alkaline solution, *Int. J. Hydrog. Energy*, 2020, **45**, 18840-18849.
30. Q. Liu, L. Yang, P. Sun, H. Liu, J. Zhao, X. Ma, Y. Wang and Z. Zhang, Ru catalyst supported on nitrogen-doped nanotubes as high efficiency electrocatalysts for hydrogen evolution in alkaline media, *RSC Adv.*, 2020, **10**, 22297-22303.

31. X. Zhang, F. Zhou, S. Zhang, Y. Liang and R. Wang, Engineering $MoS_2$ basal planes for hydrogen evolution *via* synergistic ruthenium doping and nanocarbon hybridization, *Adv. Sci.*, 2019, **6**, 1900090.
32. P. Li, X. Duan, S. Wang, L. Zheng, Y. Li, H. Duan, Y. Kuang and X. Sun, Amorphous ruthenium-sulfide with isolated catalytic sites for Pt-like electrocatalytic hydrogen production over whole pH range, *Small*, 2019, **15**, 1904043.